Journal of Molecular Catalysis A: Chemical 336 (2011) 42–50

Contents lists available at ScienceDirect

Journal of Molecular Catalysis A: Chemical

journal homepage: www.elsevier.com/locate/molcata

An easy and effective approach towards heterogeneous Pt/SiO_2-cinchonidine catalyst system for enantioselective hydrogenation of ethyl pyruvate

Muhammad Usman Azmat, Yong Guo, Yun Guo, Yanqin Wang*, Guanzhong Lu*

Key Lab for Advanced Materials, Research Institute of Industrial Catalysis, East China University of Science and Technology, 130 Meilong Road, Shanghai 200237, People's Republic of China

ARTICLE INFO

Article history:
Received 31 October 2010
Received in revised form
14 December 2010
Accepted 15 December 2010
Available online 22 December 2010

Keywords:
Heterogeneous asymmetrical catalysis
Cinchonidine functionalized SBA-15
Pt/SiO_2-CD
Enantioselective hydrogenation
Orito reaction

ABSTRACT

A single unit catalyst system (Pt/silica–chiral modifier) is developed for the enantioselective hydrogenation of ethyl pyruvate. Cinchonidine was tethered directly without prior modification over carboxylate functionalized SBA-15 by the reaction of vinyl group in cinchonidine with –COOH group in functionalized SBA-15 through ester linkage. Then Pt nanoparticles were deposited over cinchonidine tethered SBA-15. The mesostructures were characterized by small-angle XRD, N_2 sorption and TEM, while the surface functionalization was confirmed by FTIR, TG/DTA and solid state ^{13}C NMR. Enantioselectivity of the catalyst system for hydrogenation of ethyl pyruvate was determined by GC/FID. The highest enantiomeric excess was achieved as 70.8% and the catalyst recyclability was authenticated even after 3rd reuse without significant loss in enantiomeric excess.

© 2010 Elsevier B.V. All rights reserved.

1. Introduction

Growing demand of enantiomerically pure compounds in the field of life and material sciences augmented the importance of chiral synthesis [1–4]. Naturally occurring cinchona alkaloids are classified as privileged chiral catalysts [5], having unique chemical structure which can induce chirality to plenty of different achiral compounds and can yield highly pure chiral compounds [6]. The discovery of cinchona-platinum/support catalyst system for Orito reaction (Scheme 1) by the Orito's group [7,8] has initiated an avalanche of research in the field of asymmetric hydrogenation of α-functionalized activated ketones [4,9–11]. Cinchona-Pt/support chiral catalyst system has remained interestingly mysterious for more than three decades and still grabbing the attention of researchers all over the world. Since then, a variety of research works has been done which mainly focuses on the role of support [12–15], also the type of metal and its dispersity [16–21]. There is a general accord over the key role of cinchona modifier structure in the enantio differentiation reaction, which depends on the substituents at quinoline ring, quinuclidine moiety and the relative configuration of –OH group at chiral C9 position of a typical cinchona structure (Fig. 1) [22–26]. Several studies have emphasized the modifier–substrate working mechanism (1:1 adsorptive or chemical shielding model) over the metal surface [27–33] and have a point in common that tertiary N atom of quinuclidine moiety interact with the substrate molecule through either half hydrogenated or hydrogenated transition state, which controls the product around the stereogenic carbon C9. In all these studies, cinchona alkaloid was added as a modifier over Pt/support (without any chemical linkage) before the enentioselective hydrogenation reaction. The complexity in product separation and non reusability of the catalyst system make the process inefficient for industrial scale. These limitations can be eliminated by making a single unit catalyst system having chemically linked chiral modifier with the insoluble solid support in a confined environment, on to which Pt can be loaded afterwards to create a sufficient environment so that reactions should proceed enantioselectively.

Significant work has been done for the immobilization of the chiral ligands on to solid support to improve the reusability of the catalyst [34–37]. Catalyst based on cinchona grafted silica has proven to be very successful in other different reactions in addition to Orito's reaction i.e., dihydroxylation of olefin [38], Michael addition [39] and alkylation of glycine esters [40]. All the cinchona alkaloid grafted silica as discussed above, needed prior modification of the cinchona structure [41] before grafting, which involved some tedious steps, additionally use of plenty of solvents and reagents made the process expensive and not so environmentally benign.

It is thought that Orito's reaction may be favored if the acidic support (–COOH functionalized SBA-15) could help to accomplish

* Corresponding author. Tel.: +86 21 64253824; fax: +86 21 64253824.
E-mail addresses: wangyanqin@ecust.edu.cn (Y. Wang), gzhlu@ecust.edu.cn (G. Lu).

1381-1169/$ – see front matter © 2010 Elsevier B.V. All rights reserved.
doi:10.1016/j.molcata.2010.12.008

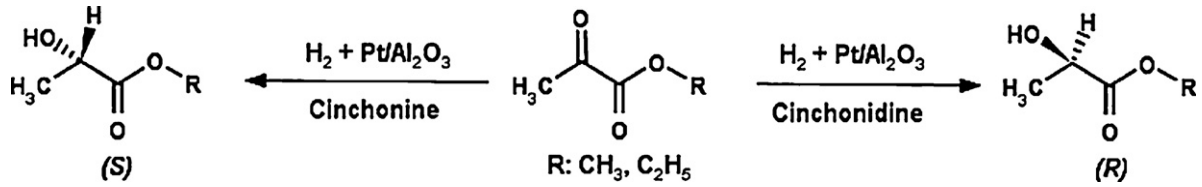

Scheme 1. Orito's reaction.

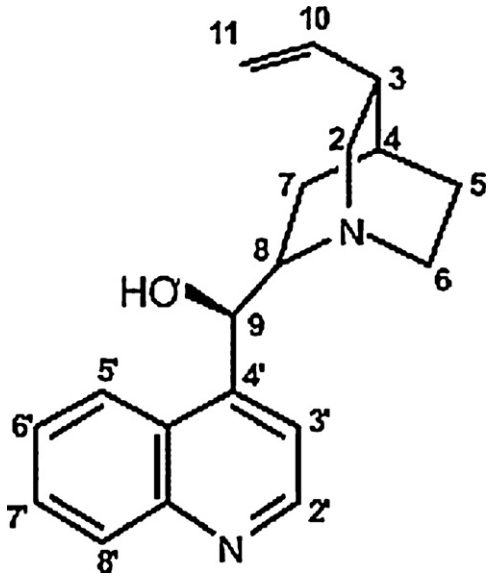

Fig. 1. Cinchonidine molecule with atomic numbering [41].

the hydrogenated modifier–substrate transition state over the Pt surface as described by different models [27–33], though this is not our mandate to discuss and prove the models here. In the present study, we mainly focused on to make the process simple and efficient by direct tethering of cinchonidine molecule within mesoporous silica frame work (SBA-15) through a spacer linker. For this purpose, firstly carboxylate functionalized SBA-15 (CA-SBA-15) having –COOH functionality extended by an ethyl group which may served as a spacer linker, was prepared. The central idea was to exploit the vinyl group present at C3 position of quinuclidine moiety in cinchonidine (Fig. 1) to tether with the carboxylate group of CA-SBA-15 through an ester linkage. Successively, Pt impregnation was employed using deposition–precipitation method over cinchonidine tethered silica (CA-SBA-CD) to achieve a new chiral catalyst system (Pt/CA-SBA-CD), probably it is only of its own kind of catalyst system studied for the enantioselective hydrogenation of ethyl pyruvate.

2. Experimental

2.1. Materials and methods

2.1.1. Reagents

All chemicals were of reagent grade and used as received. Pluronic P123 (avg. M.W. 5800) was from Aldrich Chemistry; tetraethyl orthosilicate (TEOS), p-toluene sulphonic acid (p-TsOH), acetic acid, acetonitrile, HCl, H_2SO_4, NaOH, and ethyl acetate were purchased from Shanghai Lingfeng Chemical Reagent Co. Ltd.; 2-cyanoethyl triethoxy silane (CTES) 97%, cinchonidine 99% and ethyl pyruvate 98% were purchased from Alfa Aesar.

2.1.2. Synthesis of carboxylate functionalized SBA-15 (CA-SBA-15)

Carboxylate functionalized SBA-15 was synthesized with slight modification as reported in references [42–44], which involved the first synthesis of cyano functionalized silica (CN-SBA-15) and the following hydrolysis and template removal to yield CA-SBA-15. CN-SBA-15 was synthesized by co-condensation method. The molar composition of the mixture was taken as $(1-x)$TEOS:xCTES:5.9 HCl (37%):193.0 H_2O:0.017 P123, where $x = 0.05$, 0.1, 0.15 and 0.2 (the samples are denoted as 5-CA-SBA-15, 10-CA-SBA-15, 15-CA-SBA-15 and 20-CA-SBA-15 respectively). In a typical synthesis, 3.94 g of P123 was dissolved in 160 mL of 1.7 N HCl solution at 40 °C, to this solution; calculated amount (if $x = 0.15$) 1.3 g of 2-cynoethyl triethoxy silane (CTES) was added drop wise and allowed it to pre-hydrolysis for one hour at 40 °C. After 1 h, the calculated amount, 7.08 g of tetraethyl orthosilicate (TEOS) was added slowly and allowed to hydrolyze for next 20 h with stirring at 40 °C. The product was further aged at 90 °C for 24 h without stirring. The product was filtered and washed with de-ionized H_2O and ethanol then dried at 80 °C to get 2.5 g of CN-SBA-15.

In order to remove P123 template and further hydrolysis of –CN group to –COOH to get CA-SBA-15, the previously dried 2.0 g CN-SBA-15 was taken in a round bottom flask and 240 mL of 48% H_2SO_4 was added and refluxed at 95 °C for 24 h. The brownish product was filtered carefully and washed with sufficient amount of de-ionized H_2O till the filtrate became neutral. The product was further washed with ethanol and ethyl acetate to dissolve any degraded

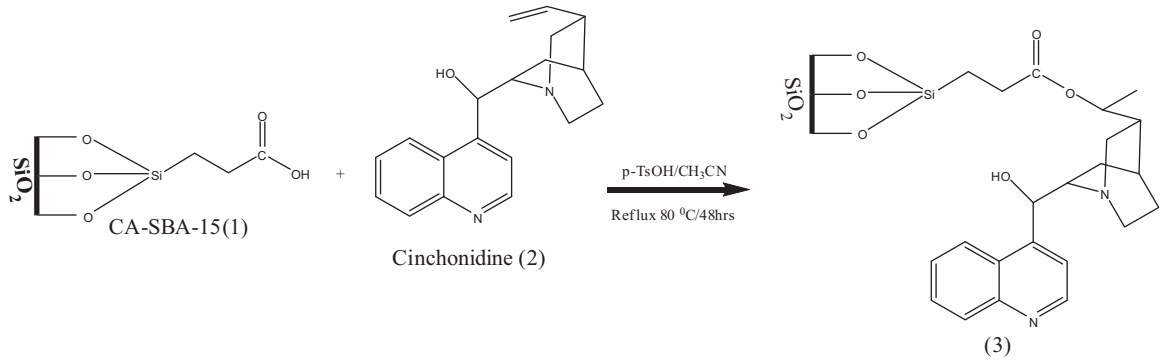

Scheme 2. Tethering of cinchonidine over CA-SBA-15 through ester linkage.

template. Finally the white product was dried at 80 °C to yield ≈0.8 g of CA-SBA-15.

2.1.3. Tethering of cinchonidine with CA-SBA-15

Scheme 2 shows the process of tethering cinchonidine (2) with the CA-SBA-15 (1) through an ester linkage by exploiting vinyl group present at C3 position of cinchonidine, which may act as an electrophile in the presence of strong acid which can undergo electrophilic substitution reaction at electron rich oxygen of –COOH group of CA-SBA-15 to yield a cinchonidine tethered compound (3).

In a typical reaction procedure, 0.1 g of p-TsOH was dissolved in 20 mL of acetonitrile. To this, 0.15 g (0.51 mmol) of cinchonidine was added and raised the temperature to 40 °C to dissolve cinchonidine. After complete dissolution of cinchonidine, 0.35 g pre-dried X-CA-SBA-15 was added to the solution and refluxed at 80 °C for 48 h. The product was filtered, washed three times with methanol and dried at 80 °C to get X-CA-SBA-CD. The product was characterized by FTIR, TG/DTA and Solid state ^{13}C CP/MAS NMR.

2.1.4. Pt Impregnation over CA-SBA-CD

The deposition–precipitation (DP) method was employed for the impregnation of Pt over X-CA-SBA-CD. In a typical method, 250 mg of X-CA-SBA-CD was dispersed in 10 mL de-ionized H_2O, then calculated amount (for 3% Pt loading) 0.5 mL of $H_2PtCl_6{\cdot}6H_2O$ solution (15 mg/mL) was added and allowed to stir for 2 h at room temperature. Adjusted the pH of the mixture to 10–12 with several drops of 2 M NaOH solution and further stirred for 2 h at room temperature. After that, 3 mL of HCHO solution (37%) was added to reduce Pt ions to Pt particles under refluxing at 100 °C for 1 h till the brownish color appeared, indicating the formation of Pt particles. The product was separated through centrifugation, washed 3 times with de-ionized H_2O and dried to achieve Pt/CA-SBA-CD catalyst system for the hydrogenation of ethyl pyruvate (EP). The same procedure for the deposition of Pt particles with different initial loadings (1, 2 and 4%) over different CA-SBA-CD supports was repeated successfully but in some cases Pt deposition failed which may be because of inefficient tethering of cinchonidine over CA-SBA-15 which may inhibit the deposition of Pt particles. We observed that tethering conditions should be optimized before the Pt particles depositions. The Pt particle size and its dispersion were analyzed by TEM.

2.1.5. Enantioselective hydrogenation of ethyl pyruvate

The hydrogenation of ethyl pyruvate was carried out in a steel reactor equipped with Teflon cylinder and a pressure gauge. In a typical hydrogenation reaction, 30 mg of Pt/CA-SBA-CD catalyst was added in the cylinder, to this, 1.5 mL of acetic acid was added as solvent and 75 μL of ethyl pyruvate was used as reactant. H_2 gas was purged several times through the cylinder and then maintained the H_2 gas pressure (0.1–0.3 MPa). The reaction was continued for 4 h at 25 °C under magnetic stirring. The enantioselective product was analyzed by GC-FID with chiral column (CHIRSSIL-DEX CB 25M × 0.25).

2.2. Characterization

X-ray powder diffraction (XRD) patterns were collected on a BRUKER D8 FOCUS using Cu Kα radiation (λ = 1.5404 Å) operated at 40 kV and 40 mA in the 2θ range of 0.8–5° at scanning rate of 0.6°/min. Nitrogen sorption isotherms were measured at 77 K using NOVA 2020e Quantachrome instrument. Each sample was evacuated at 120 °C for 8 h. The BET surface area was calculated from the adsorption branches in the relative pressure range of 0.05–0.20 and the pore volume was evaluated at a relative pressure of 0.98. The pore diameter and the pore size distribution were calculated from the desorption branch using the Barrett–Joyner–Halenda (BJH) method. The thermo gravimetric (TGA) and differential thermal (DTA) analysis were performed concurrently over PerkinElmer Pyris Diamond TG/DTA analyzer, the sample (3–5 mg) was heated in air at a rate of 10 °C/min from 40 to 800 °C. Fourier transform infrared (FTIR) spectroscopy was carried out on Nicolet Nexus 670 FTIR spectrometer with a resolution of 4 cm^{-1}, the sample was grinded with KBr and then pressed to achieve the pellets. ^{13}C CP-MAS NMR spectra were recorded on a Bruker DRX-400 spectrometer equipped with a magic angle spin probe at room temperature. Transmission electron microscopy (TEM) was performed on FEI Tecnai 20 S-TWIN operating at 200 kV. Enantiomeric excess (e.e.) for enantioselective product was calculated as e.e.% = $\{[R-S]/[R+S]\} \times 100$ and measured by GC-FID equipped with a chiral column (CHIRSSIL-DEX CB 25M × 0.25).

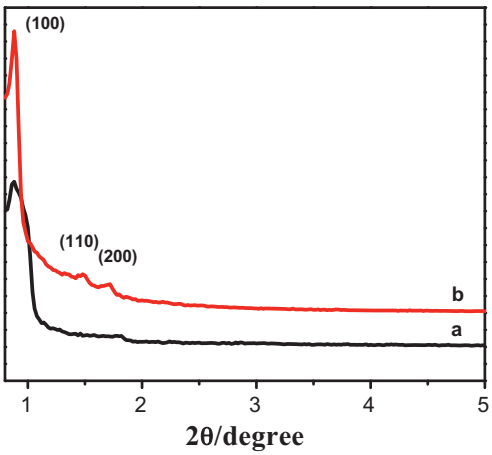

Fig. 2. Small angle XRD Patterns of (a) as-synthesized and (b) template-removed 10-CA-SBA-15.

3. Results and discussion

3.1. Surface characterization of functionalized SBA-15

Fig. 2 shows the small angle XRD patterns of as-synthesized 10-CN-SBA-15 and H_2SO_4-treated sample (10-CA-SBA-15). The characteristic reflection peaks can be assigned to (1 0 0), (1 1 0) and (2 0 0) diffractions and corresponded to the ordered 2D hexagonal space group (*p6mm*) [45,46], which confirmed the pore wall structure of SBA-15. It is obvious from Fig. 2 that the reflection peaks become better resolved and more intense for CA-SBA-15 because of the template removal from the pores. Fig. 3 shows the comparison of XRD patterns for different concentrations of carboxylate functionalized SBA-15. It can be seen that as carboxylate group concentration increases in the CA-SBA-15, the higher order reflection assigned to (1 1 0) and (2 0 0) become less intense indicating the incorporation of organic functionality $-(CH_2)_2-COOH$ in the silica framework.

Fig. 4 shows the nitrogen sorption isotherms and pore size distributions for different carboxylate functionalized SBA-15. From Fig. 4a, the N_2 sorption isotherms show sharp steps with narrow hysteresis loops corresponding to the filling of ordered mesopores. The position of the hysteresis loops shifts slightly towards lower relative pressure and the step becomes less steep as the organic contents increases in the silica frame work which indicates that the pore size decreases with an increase in –COOH contents. The pore size distribution calculated from BJH desorption branch is shown in

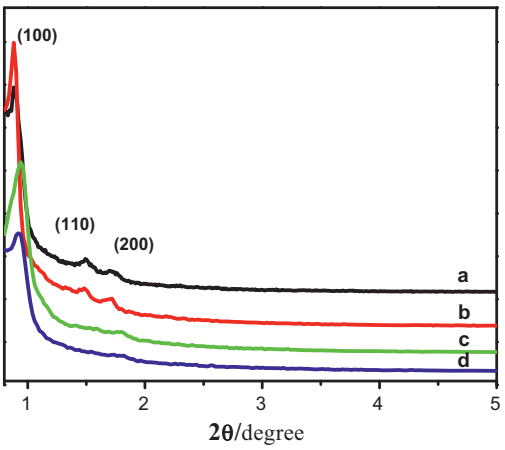

Fig. 3. Small angle XRD patterns of CA-SBA-15. (a) 5-CA-SBA-15; (b) 10-CA-SBA; (c) 15-CA-SBA-15; (d) 20-CA-SBA-15.

Table 1
Pore and surface properties of functionalized SBA-15.

Sample	Cell parameter, a_0[a]/nm	Pore diameter[b], D/nm	Surface area, SBET/$m^2\ g^{-1}$	Pore volume, $Vt/cm^3\ g^{-1}$
5-CA-SBA-15	11.6	6.2	522.3	1.19
10-CA-SBA-15	11.6	5.6	509.4	1.05
15-CA-SBA-15	10.9	5.5	503.0	0.8
20-CA-SBA-15	10.9	5.0	502.8	0.74
5-CA-SBA-CD-Pt[c]	11.6	5.9	490.3	1.04
10-CA-SBA-CD-Pt	11.6	5.5	445.9	0.98
15-CA-SBA-CD-Pt	10.9	5.5	436.8	0.78
20-CA-SBA-CD-Pt	10.9	5.0	408.6	0.68

[a] $a_0 = 2d_{100}/\sqrt{3}$.
[b] Pore diameter calculated from BJH desorption branch.
[c] X-CA-SBA-CD-Pt is functionalized SBA-15 having cinchonidine linked with X-CA-SBA-15 onto which Pt (3%, w/w) is deposited.

Fig. 4b which indicate the narrow pore size distribution for different synthesized carboxylate functionalized SBA-15.

Table 1 summarizes the pore and surface properties of functionalized SBA-15 i.e., carboxylate functionalized X-CA-SBA-15 and cinchonidine tethered CA-SBA-15 which is further deposited by Pt nanoparticles, termed as X-CA-SBA-CD-Pt. As it can be seen that pore size, BET surface area and total pore volume decreases by increasing the –COOH contents for X-CA-SBA-15. Table 1 also reveals that BET surface area and total pore volume is reduced in the same manner for X-CA-SBA-CD-Pt as for X-CA-SBA-15 due to cinchonidine tethering and Pt incorporation in the silica frame work, from these properties it can be seen that mesoporous structure remained intact for X-CA-SBA-CD-Pt even after functionalization.

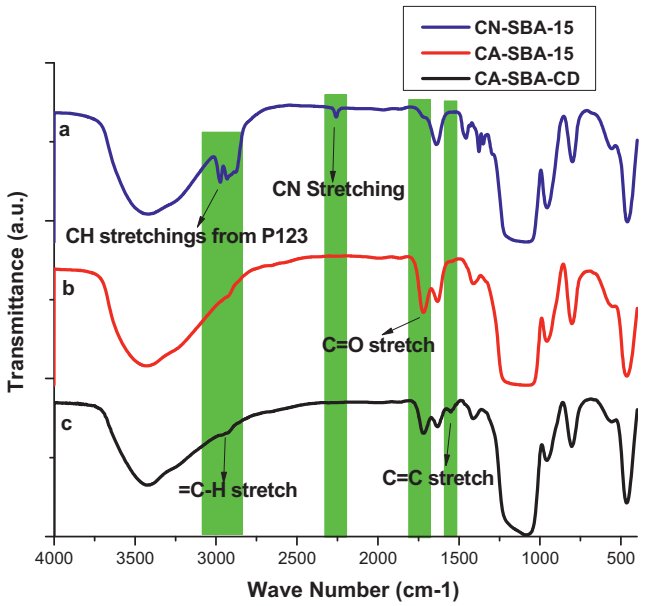

Fig. 5. A comparison of FTIR spectra for (a) as-synthesized 10-CN-SBA-15, (b) after H_2SO_4 treatment, 10-CA-SBA-15 and (c) cinchonidine tethered silica, 10-CA-SBA-CD.

3.2. Functional group characterization

Fig. 5 shows a comparison of FTIR spectra for as-synthesized 10-CN-SBA-15, after template removal and conversion of –CN to –COOH using H_2SO_4, 10-CA-SBA-15 and cinchonidine tethered carboxylate silica, 10-CA-SBA-CD. For the as-synthesized 10-CN-SBA-15 FTIR spectrum (Fig. 5, curve a) shows intense transmittance peaks of H–C–H stretching bands in the region 3000–2850 cm^{-1} and H–C–H bend due to hydrocarbon chains of the template P123 at 1464 cm^{-1}; while after treatment with H_2SO_4 (Fig. 5, curves b and c), the intense peaks disappear in the same region, indicating the removal of template. Spectrum a shows a band at 2252 cm^{-1} due to the –C≡N stretch, while the same band is found missing in the b and c spectra, which also indicate the complete conversion of –C≡N to –COOH as characteristics band for C=O stretch appears at 1720 cm^{-1}. Spectrum c shows a distinct peak at 1540 cm^{-1} due to C=C stretching vibrations along with a kink on the curve near

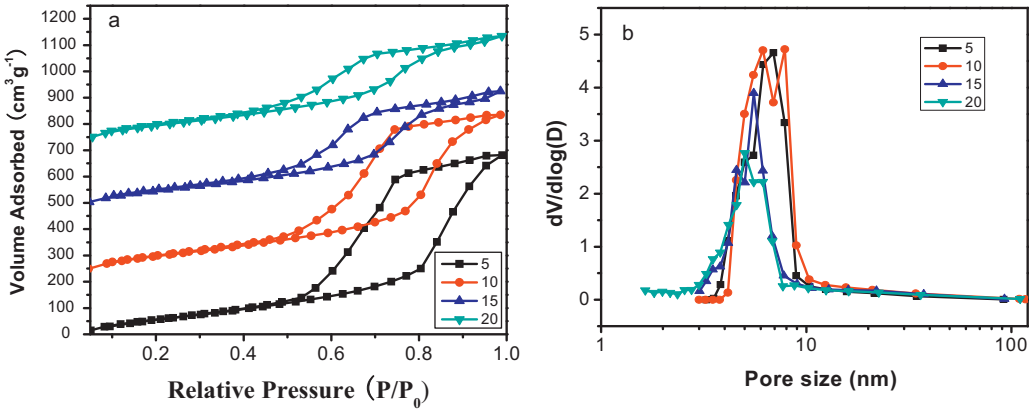

Fig. 4. Nitrogen sorption isotherms (a) and pore size distributions (b) for 5-CA-SBA-15 (■), 10-CA-SBA-15 (●), 15-CA-SBA-15 (▲) and 20-CA-SBA-15 (▼). The isotherms in (a) are shifted by 0, 250, 500 and 750 $cm^3\ g^{-1}$ STP, respectively.

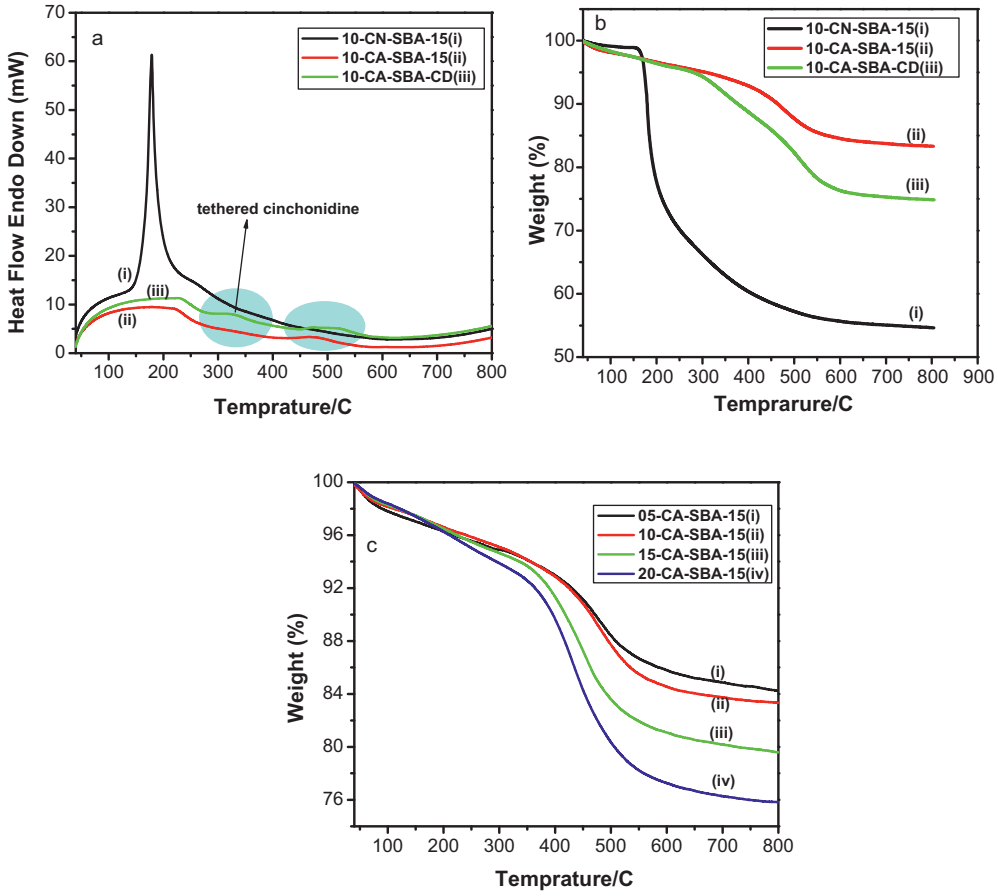

Fig. 6. Thermal analysis for different functionalized SBA-15. (a) DTA curves for 10-CN-SBA-15 (i), 10-CA-SBA-15 (ii) and 10-CA-SBA-CD (iii); (b) TGA curves for 10-CN-SBA-15 (i), 10-CA-SBA-15 (ii) and 10-CA-SBA-CD (iii) and (c) TGA curves for carboxylate functionalized SBA-15 with different –COOH contents.

3000 cm^{-1} due to aromatic = C–H stretching, which is not present in both spectra a and b, these specific bands may correspond to the aromatic ring originating from quinoline ring of the cinchonidine, hence representing the tethered cinchonidine with carboxylate SBA-15. The broad band centered at 3440 cm^{-1} is due to hydrogen bonded silanols, different interactions are possible as ≡Si–OH species may interact with each other as plain silica or with the carboxylic moieties at the surface either at the oxygen atom in the C=O or at the O–H groups [47].

Thermal analysis can also be helpful to determine the functionality on the basis of decomposition temperatures of different species incorporated in SBA-15. Fig. 6 shows TG/DTA curves for different functionalized SBA-15. For sample 10-CN-SBA-15, the DTA curve in 6a(i) shows an intense exothermic peak centered at 180 °C, which is attributed to the decomposition of the template P123; the decomposition of $-(CH_2)_2$-CN groups occurred in the temperature range of 160–500 °C, the corresponding weight loss can be calculated from TGA curve in Fig. 6b(i), i.e., 42.3%. DTA curves in Fig. 6a(ii) and (iii) show the absence of sharp intense peak at 180 °C due to the complete removal of template P123. DTA curve for 10-CA-SBA-15 (Fig. 6a(ii)) shows two prominent changes, first one is in the temperature range of 40–350 °C, from 40 to 100 °C, the weakly adsorbed moisture desorption occurs, while the strongly associated water moisture is gradually dehydrated in the temperature range of 100–350 °C [42], resulted in 5.9% weight loss as calculated from Fig. 6b(ii). The second prominent change in curve Fig. 6a(ii) is in the temperature range 350–600 °C, which is mainly attributed to the decomposition and total loss of loaded $-(CH_2)_2$–COOH groups from SBA-15, the weight loss in this temperature region is calculated as 9.6% from Fig. 6b(ii). DTA curve for cinchonidine tethered carboxylate functionalized SBA-15 shown in Fig. 6a(iii) have three temperature regions of special significances, first temperature range from 40 to 300 °C is the desorption of physically adsorbed water and dehydration of strongly associated water from the sample, the weight loss due to water calculated from Fig. 6b(iii) is 5.7%. The second temperature range from 300 to 400 °C is due to the decomposition of tethered cinchonidine which seems to overlap the third temper-

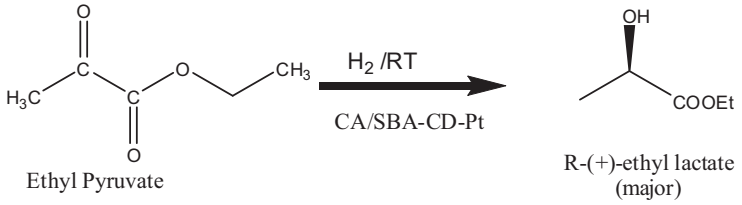

Ethyl Pyruvate

R-(+)-ethyl lactate
(major)

Scheme 3. Test reaction.

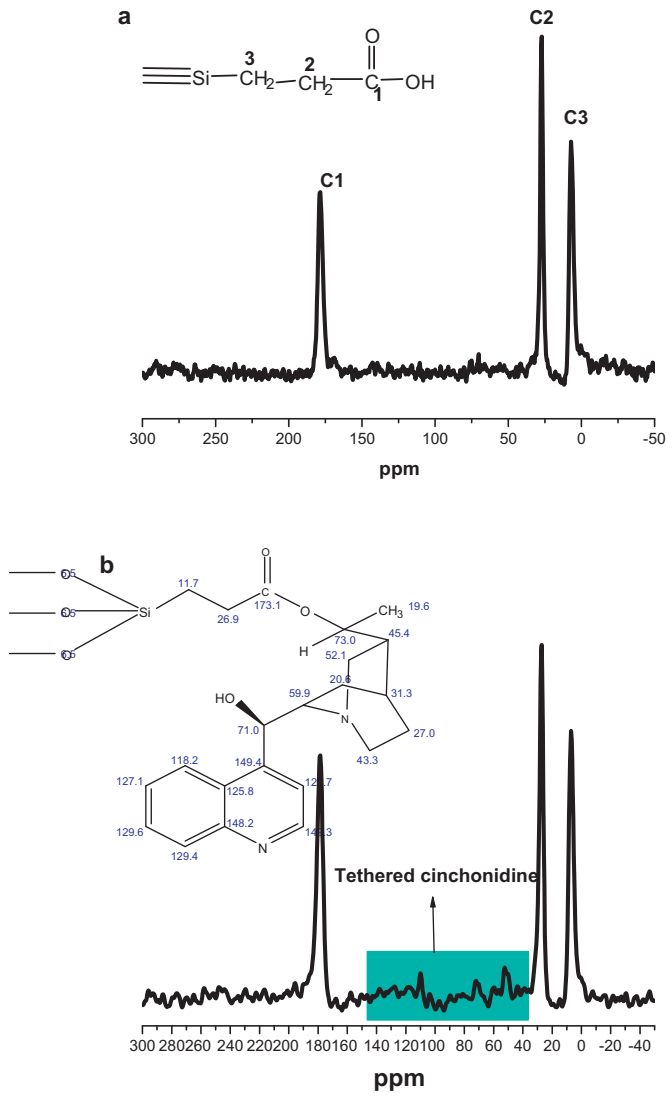

Fig. 7. ^{13}C CP/MAS NMR spectra of (a) 15-CA-SBA-15 and (b) 15-CA-SBA-CD with proposed cinchonidine tethered molecule.

ature region between 400 and 600 °C. The weight loss calculated from Fig. 6b(iii) in the temperature range 300–600 °C is 18.3%, which means 8.7% of cinchonidine is incorporated within carboxylate functionalized SBA-15, either physically or chemically tethered as proposed in Scheme 2. TGA curves for different concentrations of CA-SBA-15 (Fig. 6c) shows that percentage weight loss increases as the $-(CH_2)_2-$COOH content increases in the temperature range of 350–600 °C, corresponding to the decomposition of $-(CH_2)_2-$COOH.

To support the proposed reaction for cinchonidine tethering with carboxylate functionalized SBA-15 (Scheme 2), ^{13}C CP/MAS NMR spectroscopy was performed. Fig. 7 shows the NMR spectra of 15-CA-SBA-15 and 15-CA-SBA-CD. From Fig. 7a, it can be seen that three resonance lines of $-(CH_2)_2-$COOH groups are very distinct (as labeled at 178.6, 27.6 and 7.2 ppm with corresponding carbons), additionally there are no other lines corresponded to –CN groups or from surfactant P123, hence the simultaneous conversion of –CN group to –COOH and removal of P123 by the treatment of 15-CN-SBA-15 with H_2SO_4 is happened. It can be seen from Fig. 7b that there are some additional resonance lines other than the basic three peaks from $-(CH_2)_2-$COOH. These lines may be corresponded to the respective carbons as proposed in the Scheme 2. The chemical shifts (δ) can be identified easily from the spectrum, i.e. δ centered at 72.4 ppm is corresponded to the ester linkage carbon from vinylic group of cinchonidine, as well as overlapping with δ = 71 ppm of the C-9 of the cinchonidine linked with –OH, which shows that no ester linkage occurs at C-9. As stated earlier, due to steric hindrances and nature of –OH group (secondary alcoholic group) possibly make –OH group at C-9 position unavailable for esterification reaction with –COOH group of CA-SBA-15. Carbon atoms from quinuclidine moiety of cinchonidine can be identified from a range of low intensity peaks at 40.2, 52 and 59.8 ppm. The aromatic part of cinchonidine i.e., quinoline ring can be verified through δ 110 ppm and other low intensity lines at 118, 128.8 and 137.7 ppm. The described chemical shift is highlighted in the Fig. 7b as tethered cinchonidine. In this way, the proposed reaction suggested in Scheme 2 is true.

3.3. TEM analysis

Transmission electron microscopic (TEM) analysis was performed for different cinchonidine tethered carboxylate functionalized SBA-15, which is further impregnated by Pt particles. Fig. 8 shows TEM images of different Pt loaded (3%, w/w, based on initial loading) cinchonidine tethered carboxylate functionalized SBA-15 (Pt/CA-SBA-CD). From TEM images, it is obvious that all samples retained ordered mesoporous structure even after the functionalization, in accordance with the N_2 sorption and XRD results.

Fig. 8 also depicts that Pt particles (black spots) of ≈2 nm in size are distributed in the channels except that of Fig. 8a$_2$, which has the lowest carboxylate (–COOH) contents. Though Pt impregnation was followed by the tethering of cinchonidine, there must be some unreacted carboxylate groups. It should be mentioned here that silica functionalized with carboxylate groups has negatively charged surface in neutral to basic environments [42]. As during impregnation process NaOH is used for precipitation of $PtCl_6^{2-}$ to $Pt(OH)_2$, which can also remove the acidic H^+ from –COOH group of CA-SBA-15 to yield $-COO^-$ ion, it is very possible that thus generated $-COO^-$ can form a complex with Pt which may help to control the growth of Pt crystallites and its distribution among the pore channels of the functionalized SBA-15. One of the possible reasons for growing of Pt lumps in 05-CA-SBA-CD could be the lower number of unreacted –COOH groups which results in lesser control over Pt particles growth and its dispersion.

3.4. Enantioselective hydrogenation of ethyl pyruvate

The synthesized catalyst system Pt/CA-SBA-CD was used for the enantioselective hydrogenation of ethyl pyruvate (EP), which yield two products, i.e., R-(+)-ethyl lactate and S-(−)-ethyl lactate as shown in Scheme 3.

The optimum design of the catalyst system and the reaction conditions can provide the better enantioselectivity for the desired product, i.e., R-(+)-ethyl lactate. So, a series of experiments were performed to achieve the maximum enantiomeric excess (e.e.) and discussed below.

3.4.1. Effect of tethering conditions and –COOH functional group contents

The catalyst system Pt/X-CA-SBA-CD consists of three parts, the first part is carboxylate functionalized SBA-15 with different –COOH contents, the second part is to anchor cinchonidine through ester linkage with carboxylate functionalized silica using p-TsOH as catalyst, while the third part is the impregnation of Pt metal into the pore channels of thus functionalized SBA-15. Among these steps, tethering steps is of crucial importance as shown in Table 2.

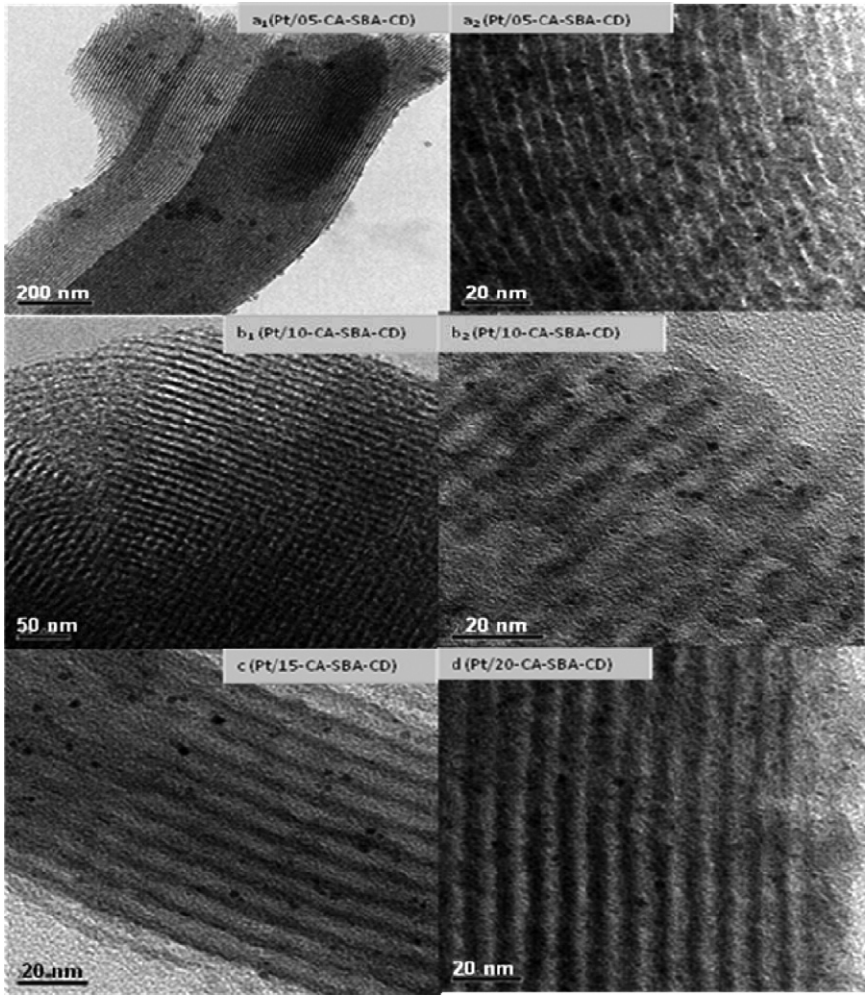

Fig. 8. TEM images of Pt/05-CA-SBA-CD (a_1 and a_2), Pt/10-CA-SBA-CD (b_1 and b_2), Pt/15-CA-SBA-CD (c) and Pt/20-CA-SBA-CD (d).

Tethering step is dependent on the ratio of cinchonidine to p-TsOH, even in some cases Pt impregnation was not successful because of inefficient tethering of cinchonidine when the ratio of cinchonidine to p-TsOH is high, which may block the pore channels and induce hydrophobicity to inhibit the deposition of Pt particles. The optimum ratio of cinchonidine to p-TsOH was found to be 1.5, which yielded the high e.e. value.

Table 2
Optimization of the tethering step.

–COOH (%)	Cinchonidine: p-TsOH (ratio)	Linkage[a] chemical/physical	e.e.% (R)
5	1	Chemical	49.2
10	2	Chemical and physical	59.8
15	1.5	Chemical	68.3
	2	Chemical and physical	63.5
20	2.5	Chemical and physical	N.T.[b]
	1.5	Chemical	60.2
	2	Chemical and physical	25.0
	3	Physical	N.T

[a] Nature of linkage is determined from TG/DTA, physically linked cinchonidine and tethered cinchonidine has different decomposition temperatures.
[b] N.T. = not tested because Pt impregnation was not successful.

Having achieved the optimum tethering condition, the effect of carboxylate group contents was investigated. Table 3 depicts the behavior of –COOH group density over silica surface towards the enantioselective hydrogenation of ethyl pyruvate. As discussed above, –COOH group (possibly not reacted with cinchonidine) increase the charge polarity of the silica surface which helps to control the homogeneity of Pt distribution. By closely observing the TEM images in Fig. 8, it is obvious that Pt particle size and distribution become more homogeneous as –COOH groups increases. For an ideal enantioselective hydrogenation reaction, there should be an environment containing Pt atoms which can provide proper orientation for ethyl pyruvate to react with H_2 molecule and cinchonidine (chiral modifier) should be in the close vicinity to induce the enantioselectivity. Though by increasing –COOH contents give better Pt distribution but smaller Pt particle size (less than 2 nm) it lessen the chances of cinchonidine (ca. 1.2 nm in size [37]) to come in the close vicinity of the Pt atoms which may result in lowering

Table 3
Effect of –COOH group density.

–COOH (%)	Conversion (%)	*R*	*S*	e.e.%
5	100	77.7	22.3	55.4
10	100	78.8	21.2	57.6
15	100	84.1	15.8	68.3
20	100	80.1	19.9	60.2

X-CA-SBA-15 = 350 mg, cinchonidine = 150 mg, P-TsOH = 100 mg, Pt loading = 3%, H_2 pressure = 0.1 MPa, temperature = room temperature (RT), reaction time = 4 h.

Table 4
Effect of H_2 pressure over enantioselectivity.

Pressure (MPa)	Conversion (%)	*R*	*S*	e.e.%
0.1	100	84.2	15.8	68.4
0.2	100	85.4	14.6	70.8
0.3	100	83.3	16.7	66.6

Catalyst (Pt/15-CA-SBA-CD) = 30 mg, Pt loading = 3%, ethyl pyruvate = 75 μL, temperature = RT, reaction time = 4 h.

the e.e. value as with the case of Pt/20-CA-SBA-CD catalyst system, this result is concurrent with literature that catalysts having Pt particle size less than 2 nm are found to be less selective [37]. The maximum e.e. value was achieved as 68.3% with Pt/15-CA-SBA-CD catalyst system because of the balanced design of the catalyst.

3.4.2. Effect of H_2 pressure

After achieving the optimum catalyst system i.e., Pt/15-CA-SBA-CD, the effect of H_2 pressure over the enantiomeric excess was determined, the results are shown in Table 4. The surface H_2 concentration may directly influence the adsorption of the reactant and thus enantioselection. From the literature [37,48–49] it is known that for different catalyst systems, H_2 dependence over enantioselection is not fixed. Webb et al. [50] reported only a slight and unsystematic variation of e.e. and a first order dependence of the rate for hydrogen pressures between 10 and 100 bar (EUROPT-1, Cd, ethanol, 25 °C). Augustine et al. [51] found that e.e.'s increased from 1% to 15% between 200 and 400 Torr, and then stayed constant until 800 Torr, while the rate was approximately first order in hydrogen pressure (Pt/A1203, HCd, methyl acetate, 25 °C).

Though in our case the reaction conditions are mild, increasing H_2 pressure (from 0.1 to 0.3 MPa) was found to have a little effect over the e.e. value, the best e.e. value was achieved 70.8% at 0.2 MPa and the least e.e. was found 66.6% at 0.3 MPa, which followed the same trend of unsystematic and slight variations as reported by Webb et al.

3.4.3. Effect of Pt loading

Pt concentration plays a very vital role in the catalyst system of Pt/15-CA-SBA-CD for enantioselective hydrogenation of ethyl pyruvate. Generally, high Pt dispersions are detrimental for high enantioselectivities; however, the optimal size of the Pt crystallites has a decisive influence on the catalytic performance [37]. As discussed earlier for a successful enantioselective reaction, there is interplay between Pt crystallites, chiral modifier and substrate molecule. If the Pt concentration (which could yield smaller particles i.e., less than 2 nm) is too low to interact simultaneously with the substrate and chiral modifier (ca. size 1.2 nm), then it could result in low yield and poor enantiomeric excess. As shown in Table 5, 1% of Pt loading gives 75% of the product and yields almost a racemic mixture with only 13% of e.e. By increasing Pt loading in the catalyst system, the better results i.e., 100% conversion and 56.6% e.e. was obtained for 2% of Pt loading, and for 3% of Pt loading, even better 70.8% e.e. with 100% conversion was reached. Further increase in Pt loading (4%) proved to be deleterious for the e.e. value, which decreased to 44.8%. At higher Pt loadings (larger particle size), it can provide 100% conversion but may lack in interaction with chiral modifier due to kinetics reasons within the confined environment of functionalized SBA-15.

Table 5
Effect of Pt loading.

Pt loading (%)	Conversion (%)	*R*	*S*	e.e.%
1	75	56.5	43.5	13
2	100	78.3	21.7	56.6
3	100	85.4	14.6	70.8
4	100	72.4	27.6	44.8

Catalyst (Pt/15-CA-SBA-CD) = 30 mg, ethyl pyruvate = 75 μL, H_2 pressure = 0.2 MPa, temperature = RT, reaction time = 4 h.

Table 6
Catalyst recyclability.

Catalyst (Pt3%-15-CA-SBA-CD)	Conversion (%)	*R*	*S*	e.e.%
Fresh	100	85.4	14.6	70.8
1st reuse	100	83.7	16.3	67.4
2nd reuse	100	82.9	17.1	65.8
3rd reuse	100	81.8	18.2	63.6

Catalyst = 30 mg, ethyl pyruvate = 75 μL, H_2 pressure = 0.2 MPa, temperature = RT, reaction time = 4 h.

3.4.4. Catalyst recyclability

Single unit catalyst is advantageous if it can provide recyclability. The catalyst can be recycled by simple centrifugation and washing thrice with acetic acid. Table 6 shows the results for catalyst reusability, the synthesized catalyst system was found to be effective after four successive reactions without sufficient decrease in e.e. value (70.8–63.6%) and with prominent catalytic activity (100% conversion). The decrease in e.e. value can be related with the shift in interaction between metal and chiral modifier in the confined environment after consecutive usage.

4. Conclusions

A catalyst system was synthesized for the enantioselective hydrogenation of ethyl pyruvate. Cinchonidine was tethered directly without prior modification over carboxylate functionalized SBA-15 using p-TsOH as catalyst through ester linkage. FTIR, TG/DTA and NMR supported the proposed mechanism. Pt was impregnated over thus synthesized functionalized SBA-15 by deposition–precipitation method, TEM images revealed that increasing –COOH contents helps to homogenize Pt dispersion and size. Pt/CA-SBA-CD catalyst system was tested for the desired reaction and found excellent in e.e. value (70.8%) with good reusability under optimum conditions.

Acknowledgements

This project was supported financially by the 973 Program of China (2010CB732300), the National Natural Science Foundation of China (No. 20973058), the Commission of Science and Technology of Shanghai Municipality (10XD1401400) and the "Excellent scholarship" of East China University of Science and Technology, China. M.U.A acknowledges the financial support from Higher Education Commission (HEC) of Pakistan for his Ph.D. studies. Authors also thank Prof. Zhenshan Hou for his valuable discussions.

References

[1] M. Tada, Y. Iwasawa, Chem. Commun. 27 (2006) 2833–2844.
[2] S.E. Gibson, M.P. Castaldi, Chem. Commun. 29 (2006) 3045–3062.
[3] J.M. Notestein, A. Katz, Chem. Eur. J. 12 (2006) 3954–3965.
[4] E. Talas, J.L. Margitfalvi, Chirality 22 (2010) 3–15.
[5] P.Y. Tehshik, N.J. Eric, Science 299 (2003) 1691–1693.
[6] K. Kacprzak, J. Gawronski, Synthesis (2001) 961–998.
[7] Y. Orito, S. Imai, S. Niwa, J. Chem. Soc. Jpn. (1979) 1118–1120.
[8] Y. Orito, S. Imai, S. Niwa, G.H. Nguyen, J. Synth. Org. Chem. Jpn. 37 (1979) 173–174.
[9] T. Mallat, E. Orglmeister, A. Baiker, Chem. Rev. 107 (2007) 4863–4890.
[10] M. Bartok, Chem. Rev. 110 (2010) 1663–1705.
[11] H.U. Blaser, M. Studer, Acc. Chem. Res. 40 (2007) 1348–1356.
[12] M. Heitbaum, F. Glorius, I. Escher, Angew. Chem. Int. Ed. 45 (2006) 4732–4762.
[13] T.J. Hall, J.E. Halder, G.J. Hutchings, R.L. Jenkins, P. Johnston, P. McMorn, P.B. Wells, R.P.K. Wells, Top. Catal. 11 (1) (2000) 351–357.
[14] U. Bohmer, K. Morgenschweis, W. Reschetilowski, Catal. Today 24 (1–2) (1995) 195–199.

[15] U. Bohmer, F. Franke, K. Morgenschweis, T. Bieber, W. Reschetilowski, Catal. Today 60 (3–4) (2000) 167–173.
[16] Y. Huang, J. Chen, H. Chen, R. Li, Y. Li, L. Min, X. Li, J. Mol. Catal. A: Chem. 170 (1–2) (2001) 143–146.
[17] H.U. Blaser, H.P. Jalett, Stud. Surf. Sci. Catal. 78 (1993) 139–146.
[18] H.U. Blaser, H.P. Jalett, D.M. Monti, J.F. Reber, J.T. Wehrli, Stud. Surf. Sci. Catal. 41 (1988) 153–163.
[19] H.P. Jalett, D.M. Monti, J.F. Reber, et al., Stud. Surf. Sci. Catal. 41 (1) (1998) 153–163.
[20] M. Bartok, Stereochemistry of Heterogeneous Metal Catalysis, Wiley, New York, 1985.
[21] J.T. Wehrli, A. Baiker, D.M. Monti, H.U. Blaser, J. Mol. Catal. 61 (2) (1990) 207–226.
[22] H.U. Blaser, H.P. Jalett, W. Lottenbach, M. Studer, J. Am. Chem. Soc. 122 (2000) 12675–12682.
[23] T. Heinz, G. Wang, A. Pfaltz, B. Minder, M. Schürch, T. Mallat, A. Baiker, Chem. Commun. 14 (1995) 1421–1422.
[24] M. Bartok, K. Balazsik, T. Bartok, Catal. Lett. 73 (2) (2001) 127–131.
[25] A. Solladie-Cavallo, C. Marsol, F. Garin, Tetrahedron Lett. 43 (27) (2002) 4733–4735.
[26] A. Pfaltz, T. Heinz, Top. Catal. 4 (3) (1997) 229–239.
[27] M. Bartok, K. Felfoldi, B. Torok, T. Bartok, Chem. Commun. (1998) 2605–2606.
[28] D. Ferri, T. Burgi, A. Baiker, Chem. Commun. (2001) 1172–1173.
[29] M. Bartok, M. Sutyinszki, K. Felföldi, G. Szollosi, Chem. Commun. (2002) 1130–1131.
[30] N. Bonalumi, A. Vargas, D. Ferri, T. Burgi, T. Mallat, A. Baiker, J. Am. Chem. Soc. 127 (2005) 8467–8477.
[31] S. Lavoie, M. Laliberte, I. Temprano, P.H. McBreen, J. Am. Chem. Soc. 128 (2006) 7588–7593.
[32] Z. Ma, F. Zaera, J. Am. Chem. Soc. 128 (2006) 16414–16415.
[33] F. Hoxha, L. Konigsmann, A. Vargas, D. Ferri, T. Mallat, A. Baiker, J. Am. Chem. Soc. 129 (2007) 10582–10590.
[34] D.E. De Vos, I.F.J. Vankelecom, P.A. Jacobs, Chiral Catalyst Immobilization and Recycling, Wiley-VCH, Weinheim, 2000.
[35] K. Ding, Y. Uozumi, Handbook of Asymmetric Heterogeneous Catalysis, Wiley-VCH, Weinheim, 2008.
[36] K. Balazsik, B. Torok, G. Szakonyi, M. Bartok, Appl. Catal. A: Gen. 182 (1999) 53–63.
[37] H.U. Blaser, H.P. Jalett, M. Muller, M. Studer, Catal. Today 37 (1997) 441–463.
[38] B.M. Kim, K.B. Sharpless, Tetrahedron Lett. 31 (21) (1990) 3003–3006.
[39] R. Alvarez, M.A. Hourdin, C. Cave, J. d'Angelo, Tetrahedron Lett. 40 (39) (1999) 7091–7094.
[40] B. Thierry, J.C. Plaquevent, D. Cahard, Tetrahedron Asymm. 14 (12) (2003) 1671–1677.
[41] A. Lindholm, P. Mäki-Arvela, E. Toukoniitty, T.A. Pakkanen, J.T. Hirvi, T. Salmi, D.Y. Murzin, R. Sjöholm, R. Leino, J. Chem. Soc., Perkin Trans. 1 (2002) 2605–2612.
[42] Y. Chia-min, Z. Bodo, S. Ferdi, Chem. Commun. (2003) 1772–1773.
[43] Y. Chia-min, W. Yanqin, Z. Bodo, S. Ferdi, Phys. Chem. Chem. Phys. 6 (2004) 2461–2467.
[44] S. Shoucang, S.C. Pui, K. Sanggu, Z. Kewu, B.H. Tan Reginald, J. Colloid Interface Sci. 321 (2008) 365–372.
[45] D.Y. Zhao, J. Feng, Q. Huo, N. Melosh, G.H. Fredrickson, B.F. Chmelka, G.D. Stucky, Science 279 (1998) 548–552.
[46] D.Y. Zhao, Q. Huo, J. Feng, B.F. Chmelka, G.D. Stucky, J. Am. Chem. Soc. 120 (1998) 6024–6036.
[47] S. Fiorilli, B. Onida, B. Bonelli, E. Garrone, J. Phys. Chem. B 109 (35) (2005) 16725–16729.
[48] Y. Sun, R.N. Landau, J. Wang, C. LeBlond, D.G. Blackmond, J. Am. Chem. Soc. 118 (1996) 1348–1353.
[49] K. Szori, M. Sutyinszki, K. Felfoldi, M. Bartok, Appl. Catal. A: Gen. 237 (2002) 275–280.
[50] G. Webb, P.B. Wells, Catal. Today 12 (1992) 319–337.
[51] R.L. Augustine, S.K. Tanielyan, L.K. Doyle, Tetrahedron: Asymm. 4 (1993) 1803–1827.